RSC Advances

PAPER

View Article Online
View Journal | View Issue

Cite this: *RSC Adv.*, 2023, **13**, 764

N-oxide ligands for selective separations of lanthanides: insights from computation†

Tongyu Liu,[a] Alexander S. Ivanov,[b] Ilja Popovs,[b] Santa Jansone-Popova[b] and De-en Jiang*[cd]

Preorganized ligands such as bis-lactam-1,10-phenanthroline (BLPhen) show unique selectivity trends across the lanthanide series, indicating the synergistic effects of both N and O donors in complexing with lanthanides. We hypothesize that by replacing amide functional groups with an N-oxide functionality would open the door to new ligand architectures with improved selectivities. To test this idea, we computationally examined mixed N,O-donor ligands containing pyridinic N and N-oxide groups and evaluated their relative aqueous La(III)/Ln(III) selectivity by computing free energy changes for the exchange reaction between the designed ligands and a reference ligand. Three novel ligands show promise as excellent extractant agents in selectively separating trivalent lanthanides. The extent of conjugation (and hyperconjugation), the complex geometry, and the electron accumulations on the two O-donors of the N-oxide groups are found to be important factors in dictating the selectivity trends.

Received 5th November 2022
Accepted 16th December 2022

DOI: 10.1039/d2ra07029d

rsc.li/rsc-advances

Introduction

Rare earth elements (REEs), including fifteen lanthanides (Ln), Sc, and Y, find broad applications in enabling many important technologies and industries.[1–6] However, they occur naturally together due to their similar properties and must be separated. Solvent extraction is the primary means to separate different lanthanides on an industrial scale.[7] Due to lanthanide contraction, most ligands prefer to bind heavier lanthanides than the lighter ones, because of the decreasing ion size traversing the series. Commercial extractants employ oxygen donors such as tributyl-phosphate (TBP),[8] diglycolamide (DGA),[9–11] and bis(2-ethylhexyl) phosphoric acid (D2EHPA).[12] Ligands with N donors such as alkylated bis-triazinyl pyridines (BTP),[13] 6,6′-bis-triazinyl-2,2′-bipyridine (BTBP),[14] and 2,9-bis-triazinyl-1,10-phenanthroline (BTPhen)[15,16] are also used.

Recently, ligands combining hard O-donor and soft N-donor atoms have been recognized as efficient extractants. One such example is 2,9-bis-lactam-1,10-phenanthroline (BLPhen)[17] that shows unparalleled selectivity for light trivalent lanthanides.[18] The rigidity of the BLPhen backbone has been shown *via* quantum chemical calculations to be an important factor influencing the selectivity of lanthanide ions.[18] First principles molecular dynamics simulations suggested a tight binding pocket between BLPhen and Ln(III).[19] Although the BLPhen ligand is a relatively new system, first examined for Am(III)/Eu(III) separation[17] in 2017 and then for Ln(III) separations[18] in 2019, what is known about the system suggests that combining O-donor and N-donor atoms could be a general strategy to design new ligands for separations of lanthanides. An innovation would be to introduce different types of N,O donors on the BLPhen framework.

N-oxide donors are common in chelate complexes of transition metals.[20] More interestingly, some pyridine-N-oxide-derived ligands have exhibited abilities to selectively coordinate to Ln(III)[21–23] or actinides[24] whose separations can provide enlightenment on Ln(III) behaviors. Moreover, computational approaches have been increasingly used to help design new ligands, including the data-driven machine learning approach.[25] Our goal here is to computationally examine new mixed N,O-donor ligands based on phenanthroline and N-oxide functionalities for complexation across the Ln(III) series, in order to gain insights into their potential for separating Ln(III)s and to correlate with their molecular structures and electronic structures in terms of key descriptors. Below we explain our computational approach first.

Computational method

It is still difficult to accurately predict the absolute binding free energy (ΔG) between a ligand and a Ln(III) ion computationally, using an implicit solvation model. By computing $\Delta\Delta G$ instead, one can focus on the overall relative trend and benefit from error cancellation. Following a previously established computational strategy,[18,26] the relative aqueous selectivity for La(III)

[a]*Department of Chemistry, University of California, Riverside, CA 92521, USA*
[b]*Chemical Sciences Division, Oak Ridge National Laboratory, 1 Bethel Valley Road, Oak Ridge, TN 37831, USA*
[c]*Department of Chemical and Biomolecular Engineering, Vanderbilt University, Nashville, TN 37235, USA. E-mail: de-en.jiang@vanderbilt.edu*
[d]*Department of Chemistry, Vanderbilt University, Nashville, TN 37235, USA*

† Electronic supplementary information (ESI) available. See DOI: https://doi.org/10.1039/d2ra07029d

over the other Ln(III) ions was evaluated by computing the Gibbs free energy change, $\Delta\Delta G_{aq}$(La/Ln), of the following ligand-exchange reaction:

$$[La(L_{ref})](NO_3)_{3(aq)} + [Ln(L_{target})](NO_3)_{3(aq)} \rightleftharpoons [La(L_{target})](NO_3)_{3(aq)} + [Ln(L_{ref})](NO_3)_{3(aq)}, \quad (1)$$

where L_{ref} and L_{target} represent the refence ligand and the target ligand (the designed one), respectively. A negative $\Delta\Delta G_{aq}$(La/Ln) means that La(III) prefers complexation with the target ligand and Ln(III) prefers the reference ligand. For the same La/Ln pair, the target ligand with more negative $\Delta\Delta G_{aq}$(La/Ln) than another target ligand would have higher La/Ln selectivity. Following the previous study,[18] we use 2,9-bis-amide-1,10-phenanthroline (BAPhen; Scheme 1) as the reference ligand.

The energies of the four 1 : 1 ligand–metal complexes in reaction (1) were computed at the B3LYP level of density functional theory (DFT) using the Gaussian 16 (revision C.01) program package.[27] 6-31+G(d) basis sets were used for the main-group elements and hydrogen. The corresponding large-core (LC) relativistic effective core potentials (RECP) were used for all lanthanides elements.[28] Frequency calculations were performed to ensure real vibrational modes for the minimum ground-state structures and to provide zero-point energies (ZPEs). ZPEs and entropy contributions (T = 298.15 K) calculated at the B3LYP/LC/6-31+G(d) level were added to the total energy to obtain the Gibbs free energies. Initial structures for geometry optimizations were generated from the corresponding experimental crystal structures by appropriately modifying donor atoms, substituents, and backbone of the BLPhen ligands. Typical input file and coordinates for converged complex structures are provided in ESI.† All calculations were performed in aqueous environment by employing the IEF-PCM (integral equation formalism of the polarizable continuum model) implicit solvation model to obtain solvation free energies in the aqueous solution.[29] To correct the errors on the free energies of low-frequency vibrational modes from the harmonic oscillator model, frequencies lower than 60 cm^{-1} were set to 60 cm^{-1} by following the quasiharmonic approximation.[30]

Results and discussion

Changing the amide groups in BLPhen to N-oxides

Our design starts with modification of the O donors on the BLPhen ligand (**1a** in Fig. 1) by replacing the amide moieties with N-oxides (**1b–1d**). Fig. 1b summarizes the computed $\Delta\Delta G$ trends across the Ln(III)s for the four ligands. One can see that the La(III)/Ln(III) selectivity becomes worse upon replacing one or both amides in **1a** with N-oxide functionality. Fig. 1b also shows an interesting peak at Ce, meaning that the target ligands (**1a–1d**) prefer to bind Ce(III) over La(III). This non-linear trend at Ce has also been observed in several experimental reports,[18,31] suggesting a different chemical nature of Ce(III) from nearby Ln(III)s.

To understand the overall performance from the N-oxides (ligands **1b-1d**), we determined the partial charges on the O donors by the natural bond orbital (NBO) populations and found the charges of −0.68*e* for **1a**, −0.64*e* for **1b**, and −0.63*e* for **1c** and **1d**. In other words, changing amide moieties to N-oxides does not make the O donors more negative, as initially hypothesized. This is likely due to the enhanced π conjugation from the pyridinium group in **1b–1d**. Hence our next strategy is to tune the conjugation to see if the performance of N-oxide-based ligands can be improved.

Tuning the conjugation of the N-oxide ligands by varying the center ring

The ligands **1a–1d** all have the conjugation throughout the whole molecule. Our idea was to disrupt the conjugation at the middle ring (**2a–2d** in Fig. 2a). Since **1b**, **1c**, and **1d** show similar performances (Fig. 1b), we selected **1d** as a starting ligand. Four

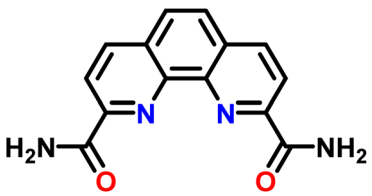

Scheme 1 The 2,9-bis-amide-1,10-phenanthroline (BAPhen) ligand, used as the reference ligand to determine free-energy change for the ligand-exchange reaction between La(III) and Ln(III).

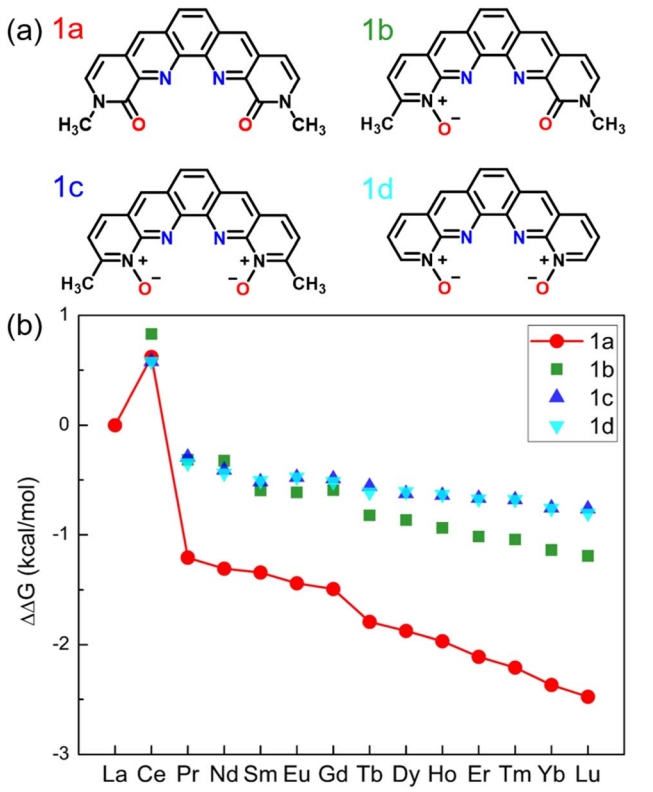

Fig. 1 (a) Chemical structures of BLPhen (**1a**) and BLPhen-derived N-oxide ligands (**1b–1d**); (b) DFT-calculated relative aqueous-phase selectivity, $\Delta\Delta G_{aq}$(La/Ln), for the ligands **1a–1d**, with respect to the refence ligand (BAPhen; Scheme 1).

new ligands were created based on modifications of **1d**: changing the middle top C=C double bond to a single bond (**2a**); reducing the middle 6-membered ring to a 5-membered ring (**2b**); enlarging the middle ring to be a 7-membered one (**2d**) or eliminating the top C=C bond (**2c**). The calculated $\Delta\Delta G_{aq}$(La/Ln) values for **2a–2d** (Fig. 2b) are compared to those of **1a**. Interestingly, ligand **2b** has much better performance than **1a**. On the other hand, the performances of **2a**, **2c**, and **2d** are worse than that of **1a**. Therefore, the reduced extent of conjugation in **2b**, combined with other factors, makes it a more selective ligand. To reveal those factors, we first compare the optimized geometries after complexation.

Similar to the structure of [La(BLPhen)]$(NO_3)_3$,[17] our optimized [La(**2b**)]$(NO_3)_3$ complex (Fig. 3) also has tenfold coordination: four donors from **2b** ligand and six from three bidentate nitrates. Both [La(**2b**)]$(NO_3)_3$ and [Ln(**1a**)]$(NO_3)_3$ complexes are planar, as evidenced by the close-to-zero O1–N1–N2–O2 dihedral angle (Table 1 and Fig. 3). On the other hand, ligands **2a**, **2c**, and **2d** are significantly non-planar, leading to less planar complexes. Therefore, the geometric comparison suggests that the planar geometry combined with the reduced conjugation helps improve the selectivity for **2b**, while the non-planarity of ligands **2a**, **2c**, and **2d** indicates that the whole conjugation is completely broken down into two smaller parts which might be detrimental to the complexation. We note that the NO_3 coordination in the Ln-complexes varies slightly from ligand to ligand.

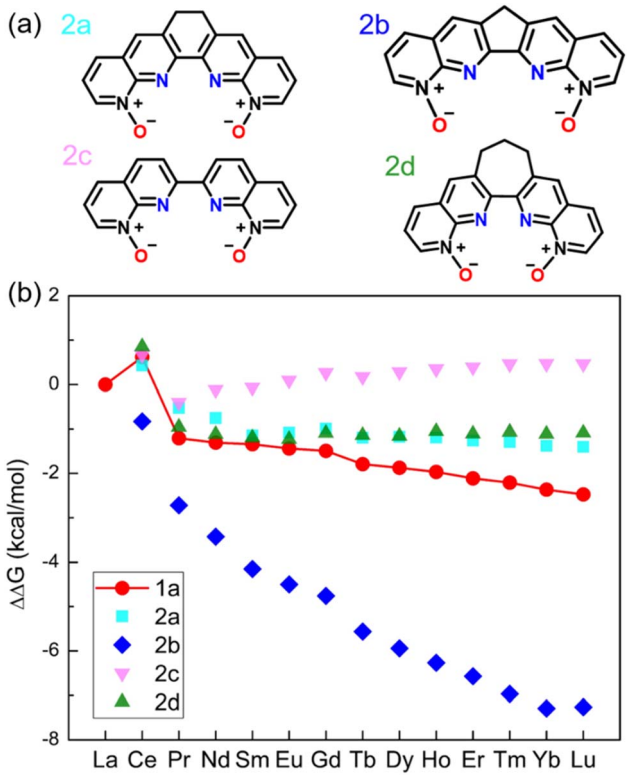

Fig. 2 (a) Chemical structures of 1,10-phenanthroline derived N-oxides with reduced conjugation. (b) DFT-calculated relative aqueous phase selectivity ($\Delta\Delta G_{aq}$(La/Ln)).

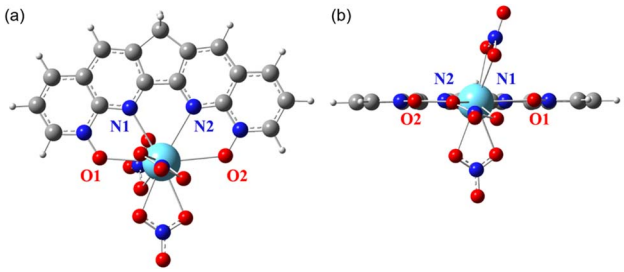

Fig. 3 DFT-optimized [La(**2b**)]$(NO_3)_3$ complex with four donors on the **2b** ligand labelled: (a) top view; (b) side view.

Unlike other ligands considered in this study, **2b** possesses a fluorene-like moiety, where the methylene group is known to be involved in hyperconjugation.[32] Indeed, our NBO analysis for **2b** revealed relatively strong interactions of the electrons in C–H σ-bonds with adjacent C=C π* orbitals (Fig. S1†) with estimated second-order stabilization energies $E^{(2)}$ of ~3.4 kcal mol^{-1}. Such hyperconjugation leads to a better geometric fit for Ln(III) ions, as reflected in the shorter Ln–N bonds in the [Ln(**2b**)]$(NO_3)_3$ complexes than in the complexes of other ligands (see Table S1† for some comparisons). On the other hand, NBO charge analyses on ligands **2a–2d** do not show significant differences of charges on pyridinic nitrogen atoms or NO oxygen atoms (Table S2†). In other words, we think that the impact of the hyperconjugation from the middle constrained 5-membered ring is more geometric than electronic.

We have further performed NBO charge analysis for [Ln(**2a**)]$(NO_3)_3$ and [Ln(**2b**)]$(NO_3)_3$ complexes (Fig. S2†) and found that the non-linear trends of Ln partial charges across the Ln series are very similar between **2a** and **2b**. The charges on Ln are lightly smaller in [Ln(**2a**)]$(NO_3)_3$ complexes than in their [Ln(**2b**)]$(NO_3)_3$ counterparts; in other words, there are more ligand charge transfers to Ln from **2a** than from **2b**. On the contrary, $\Delta\Delta G_{aq}$(La/Ln) values in Fig. 2 show that **2b** is more selective than **2a**; the selective trend across the Ln series is rather monotonic. So we conclude that the charge transfer is unlikely to be the key factor. This is consistent with our conclusion that the geometric factor is more important.

Further tuning of the conjugation size and the O–O distance of the N-oxides by varying the side rings

Since **2b** notably enhances the La(III)/Ln(III) selectivity across the whole lanthanide series, we designed additional ligands based on **2b** by modifying the conjugation size *via* the following approaches as shown in Fig. 4a: changing the two pyridiniums to five-membered rings (**3a**); changing only one outside ring to

Table 1 O1–N1–N2–O2 dihedral angles in ligands **1a**, **2a–2d** and corresponding La complexes (see Fig. 3 for the atom labels)

	1a	**2a**	**2b**	**2c**	**2d**	**3a**	**3b**	**3c**
Ligand	0.4°	9.9°	0.5°	18.9°	26.8°	0.0°	0.2°	0.6°
La(ligand)$(NO_3)_3$	0.8°	8.3°	1.3°	5.0°	14.3°	1.4°	2.0°	28.0°

a five-membered one (**3b**); inserting one phenyl ring on each side (**3c**). In comparison with **2b**, the calculated $\Delta\Delta G$ (Fig. 4b) indicates better La(III)/Ln(III) selectivity for **3a** and much worse La(III)/Ln(III) selectivity for **3c**. Considering the contrast between **3b** and **3c** in $\Delta\Delta G_{aq}$(La/Ln) values, we think that the O–O distance is a key factor here: it is too short in **3c** (Fig. 4a) which is very detrimental to the La(III)/Ln(III) selectivity. Besides geometric factors such as planarity and O–O distances, orbital interactions may also be important, which we analyze next.

Orbital and charge analyses

Computed $\Delta\Delta G_{aq}$(La/Ln) for our designed mixed N,O-donor shows that the N-oxide-based ligands **2b**, **3a**, and **3b** have the potential to be more La(III)/Ln(III) selective than the BLPhen ligand **1a**. The complexation of these ligands with Ln(III) involves mainly the donation of the lone pairs of electrons from the ligands to the Ln(III) ion. Therefore, it would be interesting to compare the HOMOs of these high-performing ligands. From Fig. 5 one can see more electron accumulation around O donors in **2b**, **3a**, and **3b** than in **1a**, which could be a reason for their improved selectivity profile. The other interesting feature is that the conjugation is similar between **1a** and **2b**, but more fragmented in **3a** and **3b**. This causes very different electron density distribution at N donors from **1a** and **2b** to **3a** and **3b**. We think that this may be the reason for the more non-linear selectivity trends across the Ln series for **3a** and **3b** (Fig. 4b).

Of course, there could be other important factors such as conjugation sizes and O–O distances discussed above, as the orbitals for all the ligands, when examined together, displays a more complicated picture (Fig. S3†). A machine-learning model that can rank all descriptors in terms of their importance in dictating the selectivity would be highly desirable. Future work is warranted.

Implications for ligand synthesis

Ligand **1a** (BLPhen) and its derivatives have been reported recently for Ln(III) separations.[17,18] Our results above suggest that the N-oxide-based **2b**, **3a**, and **3b** ligands can potentially surpass the BLPhen-based ligands. Being the simplest among the three, **2b** could be the first target and Scheme 2 shows the proposed route. It starts with a commercially available compound, 3-methyl-1,8-naphthyridine-2-carboxylic acid (**1**), which reacts with methyllithium to yield **2**,[33] followed by oxidation to **3**.[34] Equivalent **3** and 2-aminonicotinaldehyde react in potassium hydroxide and ethanol to yield **4**,[35] which dehydrates in polyphosphoric acid (PPA) to yield **5**,[36] followed by hydrazine reduction to **6**.[36] Finally, **6** can be selectively oxidized by reacting with 3.5 equivalent *meta*-chloroperoxybenzoic acid

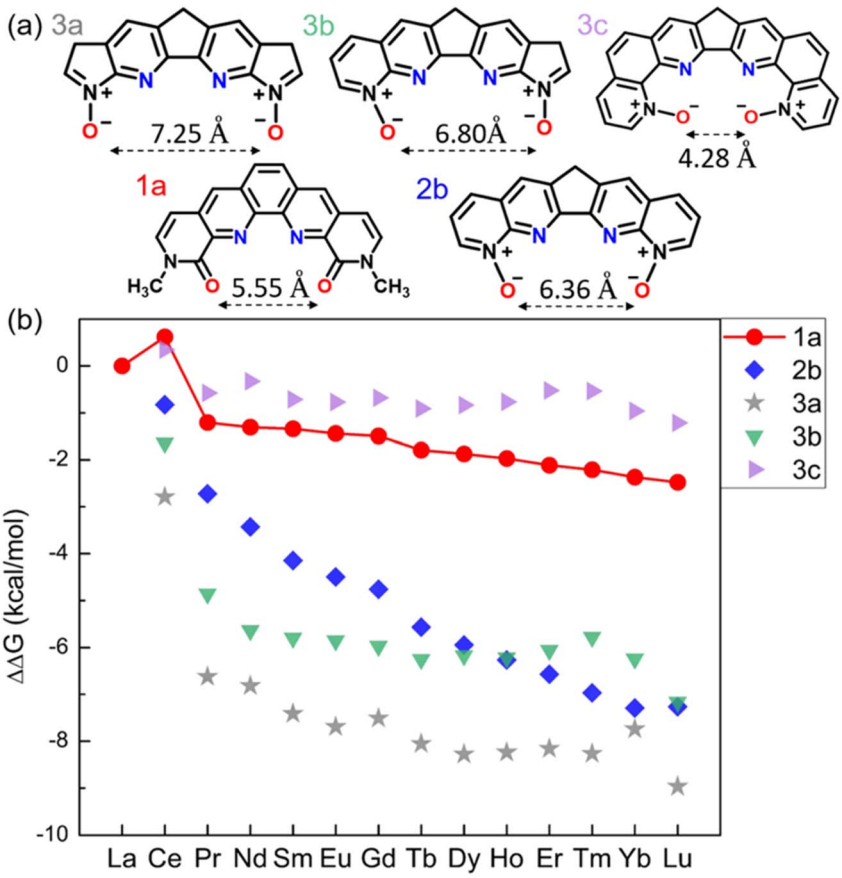

Fig. 4 (a) Chemical structures of N-oxide ligands **3a–3c** derived from **2b**; ligand **1a** is also shown for comparison in terms of O–O distance. (b) DFT-calculated relative aqueous phase selectivity, $\Delta\Delta G_{aq}$(La/Ln), for ligands **3a–3c** in comparison with ligands **1a** and **2b**.

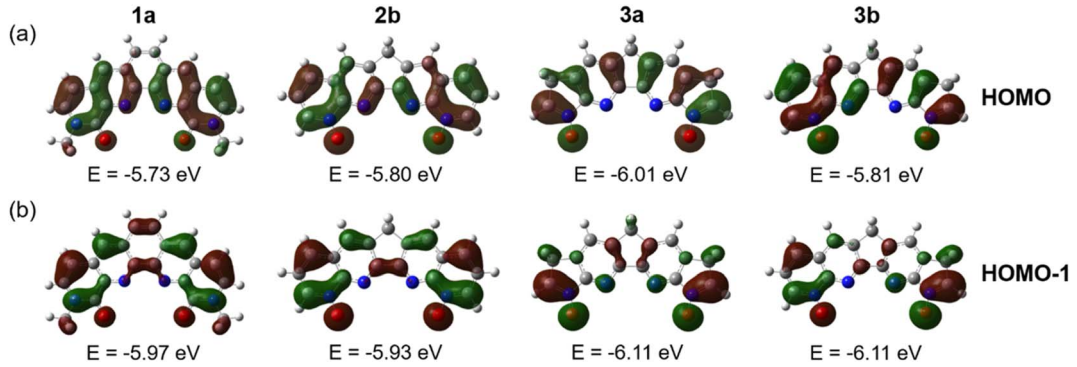

Fig. 5 (a) HOMO and (b) HOMO−1 of ligands **1a**, **2b**, **3a** and **3b** and their energies.

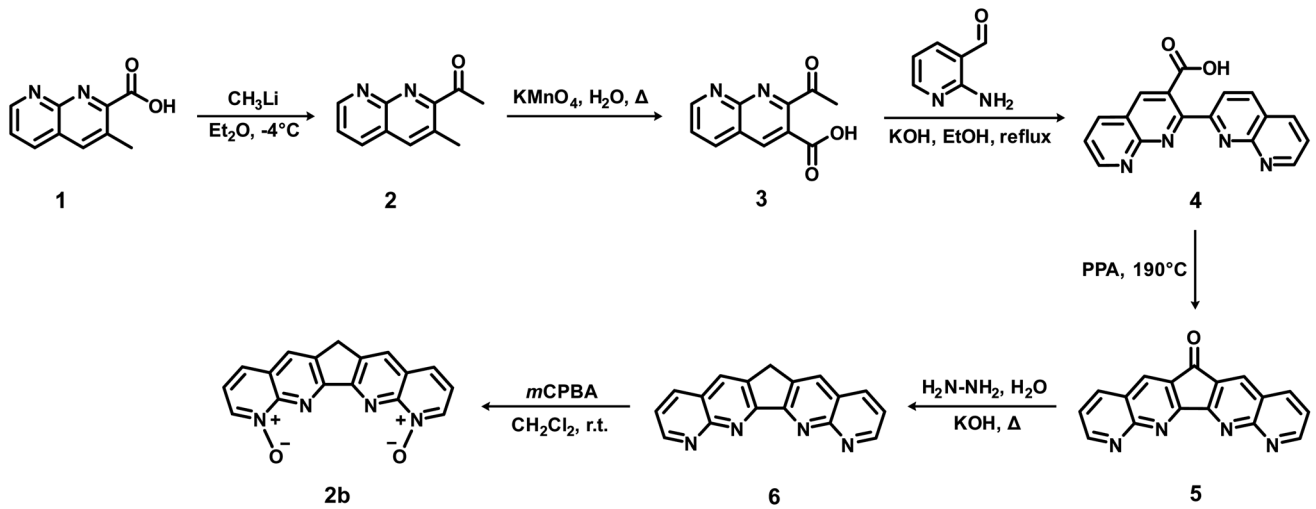

Scheme 2 Proposed route to synthesize **2b**.

(*m*CPBA) in dichloromethane,[37] to yield **2b**. Similar routes can also be adopted to synthesize **3a** and **3b**. We hope that the proposed route in Scheme 2 would inspire synthetic chemists to try it or come up with better ones.

Conclusions

We have computationally evaluated a new family of mixed N,O-donor ligands, derived from BLPhen and incorporating N-oxide functionalities, for their relative aqueous La(III)/Ln(III) selectivity. We found that the conjugation size, the O–O distance, the planarity of the formed complex, and the electron density on the two O atoms are important control knobs that affect ligand's selectivity for lanthanides. Three novel ligands (**2b**, **3a**, and **3b**) were identified to be promising and experimentally viable targets in selective separations of trivalent lanthanides. Instead of a center benzene ring as in BLPhen, the three N-oxide ligands share the feature of a center cyclopentadiene ring, which opens up the binding pocket as reflected in the greater O–O distances. The combined effect of the center cyclopentadiene ring and the N-oxide groups leads to higher predicted La(III)/Ln(III) selectivities for the designed ligands **2b**, **3a**, and **3b** than the BLPhen reference ligand. Our computational insights will guide the follow-up efforts towards synthesizing the top candidates and testing them for Ln(III) separations.

Conflicts of interest

There are no conflicts to declare.

Acknowledgements

This material is based upon work supported by the U.S. Department of Energy, Office of Science, Office of Basic Energy Sciences, Separation Science program and Materials Chemistry program under Award Number DE-SC00ERKCG21.

References

1 T. Cheisson and E. J. Schelter, *Science*, 2019, **363**, 489–493.
2 T. I. Kostelnik and C. Orvig, *Chem. Rev.*, 2019, **119**, 902–956.
3 Z. Zeng, Y. Xu, Z. Zhang, Z. Gao, M. Luo, Z. Yin, C. Zhang, J. Xu, B. Huang and F. Luo, *Chem. Soc. Rev.*, 2020, **49**, 1109–1143.

4 F. Saraci, V. Quezada-Novoa, P. R. Donnarumma and A. J. Howarth, *Chem. Soc. Rev.*, 2020, **49**, 7949–7977.
5 B. Zheng, J. Fan, B. Chen, X. Qin, J. Wang, F. Wang, R. Deng and X. Liu, *Chem. Rev.*, 2022, **122**, 5519–5603.
6 F. Ortu, *Chem. Rev.*, 2022, **122**, 6040–6116.
7 F. Xie, T. A. Zhang, D. Dreisinger and F. Doyle, *Miner. Eng.*, 2014, **56**, 10–28.
8 L. K. Sinclair, J. W. Tester, J. F. H. Thompson and R. V. Fox, *Ind. Eng. Chem. Res.*, 2019, **58**, 9199–9211.
9 E. A. Mowafy and D. Mohamed, *Sep. Purif. Technol.*, 2014, **128**, 18–24.
10 R. J. Ellis, D. M. Brigham, L. Delmau, A. S. Ivanov, N. J. Williams, M. N. Vo, B. Reinhart, B. A. Moyer and V. S. Bryantsev, *Inorg. Chem.*, 2017, **56**, 1152–1160.
11 X. He, X. Wang, Y. Cui, Z. Su, G. Ye, C. Lu and L. Li, *J. Radioanal. Nucl. Chem.*, 2021, **329**, 1019–1026.
12 A. Kumari, R. Panda, J. Y. Lee, T. Thriveni, M. K. Jha and D. D. Pathak, *Sep. Purif. Technol.*, 2019, **227**, 115680.
13 A. Kovács, C. Apostolidis and O. Walter, *Inorganics*, 2019, **7**, 26.
14 M. R. Foreman, M. J. Hudson, M. G. Drew, C. Hill and C. Madic, *Dalton Trans.*, 2006, 1645–1653.
15 Y. Yang, J. Liu, L. Yang, K. Li, H. Zhang, S. Luo and L. Rao, *Dalton Trans.*, 2015, **44**, 8959–8970.
16 D. M. Whittaker, T. L. Griffiths, M. Helliwell, A. N. Swinburne, L. S. Natrajan, F. W. Lewis, L. M. Harwood, S. A. Parry and C. A. Sharrad, *Inorg. Chem.*, 2013, **52**, 3429–3444.
17 S. Jansone-Popova, A. S. Ivanov, V. S. Bryantsev, F. V. Sloop, R. Custelcean, I. Popovs, M. M. Dekarske and B. A. Moyer, *Inorg. Chem.*, 2017, **56**, 5911–5917.
18 M. R. Healy, A. S. Ivanov, Y. Karslyan, V. S. Bryantsev, B. A. Moyer and S. Jansone-Popova, *Eur. J. Chem.*, 2019, **25**, 6326–6331.
19 T. D. N. Reddy, A. S. Ivanov, D. M. Driscoll, S. Jansone-Popova and D.-e. Jiang, *ACS Omega*, 2022, **7**, 21317–21324.
20 J. Quagliano, J. Fujita, G. Franz, D. Phillips, J. Walmsley and S. Tyree, *J. Am. Chem. Soc.*, 1961, **83**, 3770–3773.
21 I. Binyamin, S. Pailloux, E. N. Duesler, B. M. Rapko and R. T. Paine, *Inorg. Chem.*, 2006, **45**, 5886–5892.
22 M. A. S. Goher and F. A. Mautner, *J. Mol. Struct.*, 2007, **846**, 153–156.
23 H.-J. Zhang, R.-H. Gou, L. Yan and R.-D. Yang, *Spectrochim. Acta, Part A*, 2007, **66**, 289–294.
24 D. Das, M. Joshi, S. Kannan, M. Kumar, T. K. Ghanty, A. S. Pente, A. Sengupta and C. P. Kaushik, *Polyhedron*, 2021, **201**, 115166.
25 T. Liu, K. R. Johnson, S. Jansone-Popova and D.-e. Jiang, *JACS Au*, 2022, **2**, 1428–1434.
26 A. S. Ivanov and V. S. Bryantsev, *Eur. J. Inorg. Chem.*, 2016, **2016**, 3474–3479.
27 M. J. Frisch, G. W. Trucks, H. B. Schlegel, G. E. Scuseria, M. A. Robb, J. R. Cheeseman, G. Scalmani, V. Barone, G. A. Petersson, H. Nakatsuji, *et al.*, *Gaussian 16 (revision C.01)*, Gaussian, Inc., Wallingford CT, 2016.
28 M. Dolg, H. Stoll and H. Preuss, *J. Chem. Phys.*, 1989, **90**, 1730–1734.
29 J. Tomasi, B. Mennucci and R. Cammi, *Chem. Rev.*, 2005, **105**, 2999–3094.
30 R. F. Ribeiro, A. V. Marenich, C. J. Cramer and D. G. Truhlar, *J. Phys. Chem. B*, 2011, **115**, 14556–14562.
31 J. Dehaudt, N. J. Williams, I. A. Shkrob, H. Luo and S. Dai, *Dalton Trans.*, 2016, **45**, 11624–11627.
32 R. Baker, C. Eaborn and J. Sperry, *J. Chem. Soc.*, 1962, 2382–2385.
33 G. M. Rubottom and C. Kim, *J. Org. Chem.*, 1983, **48**, 1550–1552.
34 G. K. Wagner, D. Kotschenreuther, W. Zimmermann and S. A. Laufer, *J. Org. Chem.*, 2003, **68**, 4527–4530.
35 B. Xiong, S. Zhang, H. Jiang and M. Zhang, *Org. Lett.*, 2016, **18**, 724–727.
36 M. E. Hoque, R. Bisht, A. Unnikrishnan, S. Dey, M. M. Mahamudul Hassan, S. Guria, R. N. Rai, R. B. Sunoj and B. Chattopadhyay, *Angew. Chem., Int. Ed.*, 2022, **61**, e202203539.
37 R. P. Thummel and Y. Jahng, *J. Org. Chem.*, 1985, **50**, 3635–3636.